COUPLING HIGH FIDELITY BODY MODELING WITH NON-KEPLERIAN DYNAMICS TO DESIGN AIM-MASCOT-2 LANDING TRAJECTORIES ON DIDYMOS BINARY ASTEROID

F. Ferrari, M. Lavagna

Politecnico di Milano
Department of Aerospace Science and Technology
Via La Masa 34
20156 Milano, Italy

I. Carnelli

European Space Agency
General Study Program Office
8-10 rue Mario Nikis
75738 Paris Cedex 15, France

ABSTRACT

The Asteroid Impact Mission (AIM) includes among its primary objectives the release of a lander (MASCOT-2) on the surface of the smaller asteroid of binary couple 65803 Didymos. The work here presented is performed under ESA contract, in the frame of phase A mission design of AIM spacecraft. The paper focuses on the landing-related part of the design and presents the on-going work concerning the release strategy adopted to fulfill mission design requirements. The dynamics of the spacecraft are modeled using the most up-to-date gravity model of Didymos system, based on shape models of the two asteroids. Descent trajectories are selected by exploiting manifold dynamics associated to the peculiar three-body environment in the proximity of Didymos.

Index Terms— Binary asteroid, non-Keplerian dynamics, ballistic landing, AIM, three-body problem

1. INTRODUCTION

The Asteroid Impact Mission (AIM) [1, 2, 3] is a mission by ESA, planned to be the first to rendezvous with a binary asteroid. AIM mission objectives includes both scientific investigations and technological demonstrations. The mission is part of the Asteroid Impact & Deflection Assessment (AIDA) [4, 5, 6], a joint cooperation between ESA and NASA, devoted to assess the effectiveness in deflecting the heliocentric path of a threatening Near Earth Asteroid (NEA) for planetary defense purpose. The target of the mission is near-Earth binary asteroid 65803 Didymos [7], whose asteroids are informally called Didymain (bigger asteroid) and Didymoon (smaller asteroid). The goal of AIDA is to study the effects of a kinetic impact on the surface of Didymoon. To this purpose, together with AIM, the AIDA mission includes DART (Double Asteroid Redirection Test) [8, 9, 10], the kinetic impactor, designed by NASA.

The primary objectives of AIM include the detailed study and characterization of the binary couple. Among these, the internal composition of the smaller asteroid will be determined by means of low frequency radar tomography. Similarly to what done with the CONSERT instrument [11], on board the ESA's Rosetta mission [12], the radar will include a lander-orbiter architecture to host both transmitters and receivers. Rosetta mission highlighted the challenges of designing close proximity trajectories and to land a probe on the surface of an extremely irregular body such as comet 67P/Churyumov-Gerasimenko [13], whose shape and mass distribution were completely unknown and unexpected during the mission design phase. In that case, the Philae lander [14] release was challenged by the highly perturbed dynamical environment in the proximity of the comet and its very low and irregular gravity field. In analogy with the Rosetta mission, AIM will deploy a small and passive probe (MASCOT-2, with clear heritage from MASCOT [15], on board the Hayabusa 2 mission [16]) that will reach the surface of a largely unknown object after a purely ballistic descent. MASCOT-2 lander does not feature any anchoring mechanism and this makes the release even more challenging since Didymos system's gravity field is expected to be weaker, with an escape velocity from Didymoon's surface of about 4-6 cm/s, being the asteroids estimated to be nearly two orders of magnitude less massive than comet 67P/Churyumov-Gerasimenko. In addition, the presence of two gravitational attractors makes the gravity field in the close proximity of the couple highly unstable and chaotic.

The paper proposes an effective strategy for MASCOT-2 release, beneficial for the mission analysis and operations design points of view. The AIM scenario is presented as a perfect case of study, but the methodology applies to any asteroid/small body scenario. In particular, the landing trajectory and dynamics of MASCOT-2 is studied during close-proximity operations using the highest up-to-date fidelity model of Didymos. The paper presents some updates on the work the authors are currently performing during the phase A/B1 design of AIM, under ESA contract [17, 18, 19], in consortium with OHB System AG, and Spin.Works. From the orbital mechanics point of view, the binary system is naturally modeled as a three-body system and solutions are

studied within the frame of the Restricted Three-Body Problem modeling. Shape-based models are used to model the gravitational contribution of the two asteroids refined models are built by combining them to reproduce the gravity field in the proximity of the binary couple. The purpose of the design strategy is to take advantage of the presence of two gravitational attractors to find effective landing solutions. The increased complexity because of the two gravity sources is here read as a potential opportunity to be exploited through the three-body problem modeling, which opens to a variety of dynamical solutions not available whenever a single attractor is dealt with. Three-body solutions are computed for Didymos binary system and suitable trajectories to land MASCOT-2 on the surface of the secondary are selected. More in detail, the motion close to the Lagrangian points is exploited: stable manifolds associated to Halo and Lyapunov orbits, have been propagated in the high-fidelity dynamical environment and suitable solutions are selected to guarantee soft landing on the secondary asteroid. The dynamics of the lander is propagated from release up to rest on the surface of the asteroid.

2. MASCOT-2 DYNAMICS

This section discusses the model in use to reproduce the dynamics of MASCOT-2 lander. The modeling strategy is based on a modified Circular Restricted Three-Body Problem (CR3BP) formulation. Although most of the working assumptions included in the CR3BP are kept, a different model of the gravity field produced by the two asteroids is implemented. Section 2.1 introduces the basics on the classical CR3BP formulation, section 2.2 discusses the implementation of the gravitational effect due to the asteroids and finally, section 2.3 presents the modified CR3BP in use to model the dynamics of MASCOT-2 lander.

2.1. Circular Restricted Three-Body Problem

The *restricted* three-body problem describes the motion of a third body, which moves under the gravitational attraction of two massive bodies (called primaries), but does not influence their motion. Hence, the two primaries follow a two-body solution around the barycenter of the system. More in detail, in the *circular* problem, the primaries are constrained to move on circular orbits. All three bodies are modeled as point masses and their dynamics is exhaustively represented by the motion of their center of mass.

2.1.1. Equations of motion

Equations of motion of the third particle are often expressed in nondimensional form, with respect to a non-inertial frame, which rotates together with the primaries [20]. In this frame the primaries (referenced as P_1 and P_2) lie on the x axis and have fixed position: P_1=($-\mu$,0,0) and P_2=($1-\mu$,0,0), where μ is the mass ratio between the two primaries, defined as

$$\mu = \frac{M_2}{M_1 + M_2} \tag{1}$$

with M_1 and M_2 being the masses of the primaries and $M_1 > M_2$. It is known that the nondimensional form of the equations of motion depends only on parameter μ, and can be written as

$$\begin{cases} \ddot{x} = x + 2\dot{y} + U_{1_x} + U_{2_x} \\ \ddot{y} = y - 2\dot{x} + U_{1_y} + U_{2_y} \\ \ddot{z} = U_{1_z} + U_{2_z} \end{cases} \tag{2}$$

where the subscript $(\cdot)_x$, $(\cdot)_y$ or $(\cdot)_z$ indicate partial derivatives, and U_1 and U_2 represent the nondimensional point mass gravitational potential due to P_1 and P_2

$$U_1 = \frac{1-\mu}{r_1} \tag{3}$$

$$U_2 = \frac{\mu}{r_2} \tag{4}$$

with r_1 and r_2 being the distance between the body and the two primaries

$$r_1 = \sqrt{(x+\mu)^2 + y^2 + z^2} \tag{5}$$

$$r_2 = \sqrt{(x-(1-\mu))^2 + y^2 + z^2} \tag{6}$$

CR3BP solutions of interest for the case of study are recalled and used in section 3. The interested reader can refer to [20, 21, 22] for further detail on CR3BP formulation, its dynamical properties and solutions.

2.2. Asteroid shape-based gravity models

As mentioned, a modified version of the CR3BP is implemented to model the dynamics of MASCOT-2 as it moves in the proximity of Didymos binary system. More in detail, the two asteroids are modeled using shape-based models, instead of being considered as single point masses.

The most up-to-date model of Didymos system include a polyhedral shape model for Didymain and an ellipsoidal shape model for Didymoon. The following paragraphs describes briefly the strategy in use to reproduce the asteroids gravity field based on these shape models.

2.2.1. Didymain: constant density polyhedron

The gravity effect of Didymain is modeled using its shape model[1] and its mass distribution is considered to be uniform (constant density polyhedron). The derivation is based on the method proposed by Werner and Scheeres [23]. In this case, the potential function U_{poly} indicates the exact potential due

[1]The Didymain shape model is used in the frame of the AIM contract, however it is still unpublished (courtesy of L. Benner and S. Naidu)

to the shape model, as sum of the contribution due to all faces and edges of the polyhedron:

$$U_{\text{poly}} = -\frac{1}{2}G\rho\Bigg(\sum_{f\in faces} \mathbf{r}_f\cdot\mathbf{F}_f\cdot\mathbf{r}_f \cdot \omega_f - \sum_{e\in edges} \mathbf{r}_e\cdot\mathbf{E}_e\cdot\mathbf{r}_e \cdot L_e \Bigg) \tag{7}$$

where G is the universal gravitational constant, ρ is the density, $\mathbf{F}_f$ and $\mathbf{E}_e$ are dyads associated to faces and edges of the polyhedron model, $\mathbf{r}_f$ and $\mathbf{r}_e$ are vectors from the field point to faces or edges, L_e is the potential of a wire associated to the edge e and ω_f is the solid angle associated to the face f, when viewed from the field point.

2.2.2. Didymoon: constant density ellipsoid

Concerning Didymoon, the most updated model of its shape consider it as an ellipsoid. Accordingly, its gravity effect is modeled using the potential of a constant density tri-axial ellipsoid. The implementation is based on the method proposed by Scheeres [24]. The potential in the external region of the ellipsoid with semi-axes α, β, γ, aligned respectively to the x, y and z axes of the reference frame, and with $\alpha \geq \beta \geq \gamma$, can be written as

$$U_{\text{ell}} = G\rho\pi\alpha\beta\gamma \int_{\lambda(x,y,z)}^{\infty} \Phi(x,y,z;u)\frac{du}{\Delta(u)} \tag{8}$$

with

$$\Phi(x,y,z;u) = \frac{x^2}{\alpha^2+u} + \frac{y^2}{\beta^2+u} + \frac{z^2}{\gamma^2+u} - 1 \tag{9}$$

$$\Delta(u) = \sqrt{(\alpha^2+u)(\beta^2+u)(\gamma^2+u)} \tag{10}$$

and with the parameter λ being solution of

$$\Phi(x,y,z;\lambda(x,y,z)) = 0 \tag{11}$$

2.3. Modified CR3BP

As mentioned, the dynamics of MASCOT-2 are computed using a modified CR3BP formulation. The equations of motion are modified to include the effects of non-spherical mass distribution of the two primaries: point mass potentials are replaced by shape-based potentials in Eq. 2. Modified nondimensional equations of motion read as follows

$$\begin{cases} \ddot{x} = x + 2\dot{y} + U_{\text{poly}_x} + U_{\text{ell}_x} \\ \ddot{y} = y - 2\dot{x} + U_{\text{poly}_y} + U_{\text{ell}_y} \\ \ddot{z} = U_{\text{poly}_z} + U_{\text{ell}_z} \end{cases} \tag{12}$$

Note that only the gravity terms due to the two primaries, acting on the third body have been modified. No changes have been made on the assumptions regarding the motion of the center of mass of the two primaries and their mutual interaction. Concerning the rotation motion of Didymoon, it is known that the secondary is in a tidally-locked configuration, such that it shows always the same face to Didymain and it is aligned to it along its smaller principal axis of inertia.

3. MASCOT-2 RELEASE STRATEGY

MASCOT-2, as its predecessor MASCOT (on board the Hayabusa mission), is a completely passive probe. It does not have any device to stop or anchor on Didymoon's surface once there. Also, MASCOT-2 does not have any orbit-controlling device, such as thrusters. For this reason, the landing trajectory must be carefully designed, and a well-designed purely ballistic descent is the only chance to reach Didymoon's surface. The success of the landing is completely committed to the choice of the release condition. Moreover, the safety of AIM spacecraft must be ensured during all phases of the mission, meaning that the release point shall be far enough from both asteroids. Given those requirements, the major challenge related to the MASCOT-2 landing design appears clearly linked to whether the lander will stay on the surface after touch down or not. The extremely low-gravity environment on the surface of Didymoon will likely induce the probe to bounce until reaching a stable position on Didymoon's surface or, in the worst condition, to escape from the asteroid's gravity field. The lander shall be put on a suitable trajectory, that allows the lander to safely reach Didymoon with a sufficiently small touch down velocity, such not to be bounced away. From the designer point of view, the touch down velocity plays a major role, especially when compared to the local escape velocity at the asteroid surface.

In order to better understand the dynamical behavior of the third body in such peculiar environment, it is worth to highlight the role of the escape velocity for the case of study. In the frame of the classical restricted two-body problem, the escape velocity is defined as the minimum velocity to escape from the gravitational attraction of such body. In that case, the limiting condition corresponds to the velocity to be inserted on a parabolic arc, which reaches the Sphere Of Influence (SOI) of the attractor after infinite time. Conversely, this means that a body release at the SOI, heading towards the attractor through a pure ballistic descent, will reach its surface with a touch down velocity greater or equal than the minimum escape velocity. This imposes a dynamical constraint to the minimum touch down velocity reachable from outside the SOI. As mentioned, this is valid for the case of restricted two-body problem formulation. However, analogous concepts can be derived for the case of restricted three-body problem. The restricted three-body problem is known to admit no analytical solutions to the equations of motion, but it is common to look at the qualitative behavior of the motion of the third body using the energy approach. More in detail, zero relative velocity surfaces (or) can be derived to qualitatively

bound the motion of the particle in the proximity of the two primaries (see [20, 21] for further detail). Interesting insights on MASCOT-2 scenario can be derived by following this approach. Analogously to the two-body case, it is possible to define the escape velocity as the minimum velocity allowing a massless body to escape from Didymoon's surface. For a sufficiently low amount of energy, zero relative velocity surfaces will separate clearly the region near P_1 from the region near P_2: in this case, a particle near P_2 is trapped to stay in its neighborhood. For a higher energy level, a connection between the two zero relative velocity surfaces appears in correspondence of the L1 point: in this case, the particle is allowed to move between P_1 and P_2 regions, by passing through the L1 neck. With relation to MASCOT-2 scenario, this condition can be seen as the lowest energy for a particle to escape from Didymoon's neighborhood. More in detail, the lowest energy trajectory to escape from P_2 region is the stable manifold associated to L1 point. The velocity at intersection between the manifold and the surface of Didymoon corresponds to the minimum escape velocity from Didymoon's surface. This kind of information can be used to assess the existence of a ballistic landing trajectory, from outside the P_2 region. With analogy to the escape problem, a lander can reach the surface from L1 through its unstable manifold. Both landing and escaping trajectories are found at the same level of energy, corresponding to the opening of the L1 neck. It is known that a higher level of energy allows the opening of the L2 neck. In this case, the particle has enough energy to escape from the attraction of both asteroids.

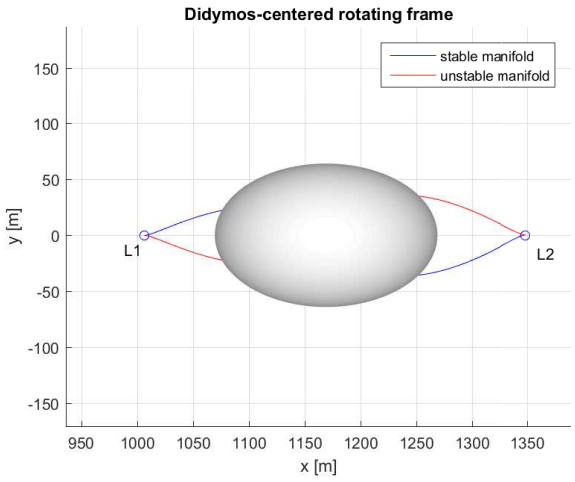

Fig. 1. Stable (blue) and unstable (red) manifolds associated to L1 and L2 points. Stable manifolds corresponds to minimum escape velocity solutions, unstable manifolds to minimum touch down velocity solutions

The L1 case is the lower limiting case in terms of energy level of the third body. This solution might be applied to the MASCOT-2 scenario. However, due to safety issues, the L1 solution is discarded in favor to a safer release from L2 side. It is indeed preferable to release the lander from outside the asteroid system (L2 side) rather than from between the two asteroids (L1 side). For these reasons, for MASCOT-2 scenario, low energy trajectories associated to unstable manifold of L2 are investigated as suitable landing solutions. Figure 1 shows the stable/unstable manifold branches associated to L1 and L2, corresponding respectively, to minimum escape/touch down velocity solutions.

A purely ballistic landing can be achieved by releasing MASCOT-2 from the L2 point, on its unstable manifold. This constraints the release altitude and the AIM spacecraft trajectory to the L2 point. Different and higher release altitudes are desirable from the mission design point of view. To achieve this goal, a ballistic transfer can be constructed from outside the L2 region, by combining stable L2 manifold (from release point up to L2) with unstable manifold (from L2 to Didymoon's surface).

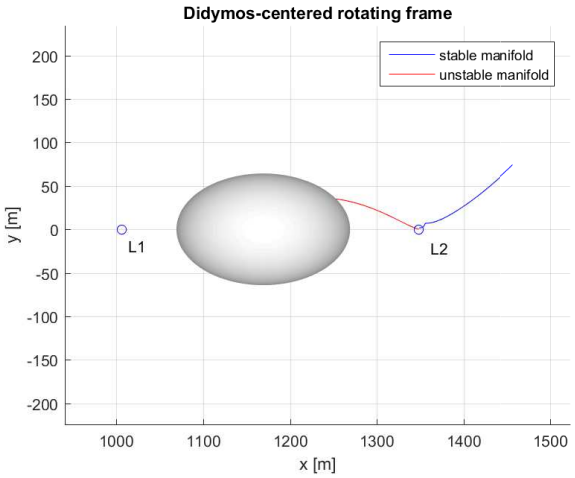

Fig. 2. Stable (blue) and unstable (red) manifolds associated to L2 point. Stable manifold branch carries the lander from release point up to L2, where it jumps on the unstable branch to proceed towards the Didymoon's surface

The complete ballistic path of MASCOT-2 from release up to touch down is shown in Figure 2. It is here highlighted that manifolds are firstly computed using the classical CR3BP formulation. This result is then used as initial condition for the dynamical propagation using the modified CR3BP model described in section 2.3.

4. DYNAMICS AFTER TOUCH DOWN

An important part of MASCOT-2 landing design is to assess and simulate the dynamics of the lander once it gets in contact with the asteroid's soil. The interaction with Didymoon's surface is a crucial point to establish whether MASCOT-2 will

escape or not after bouncing. More in detail, the most important point is to assess the quantity of energy dissipated at touch down. This effect can be summarized into a single parameter, called restitution coefficient, defined as the ratio between velocity after (v_{TD}^{+}) and before (v_{TD}^{-}) touch down

$$\eta = \frac{v_{\text{TD}}^{+}}{v_{\text{TD}}^{-}} \tag{13}$$

The restitution coefficient ranges from 0 (fully inelastic collision) to 1 (fully elastic collision) and it represents a measure of the energy dissipated at contact. As for the case of study, two different effects are considered as dissipative terms: part of the energy at touch down will be absorbed by the structure of MASCOT-2 (η_{struct}), part of it will be absorbed by the asteroid's soil (η_{soil}):

$$\eta = \eta_{\text{struct}} \cdot \eta_{\text{struct}} \tag{14}$$

The restitution coefficient allows to evaluate the amount of energy dissipated by the impact, which essentially turns into a decrease in the norm of the velocity vector after bouncing. In addition, uncertainties on the local soil inclination are also included, to stochastically model the irregularities of the surface, leading into a non-trivial definition of the direction of the velocity vector after bouncing.

5. MASCOT-2 LANDING RESULTS

As motivated in section 3, baseline design strategy considers the release of MASCOT-2 on a stable manifold associated to L2, and a transition at L2 to the unstable manifold branch to reach Didymoon's surface. More in detail, suitable solutions are selected, with considering different release altitude. The robustness of the ballistic landing solution is validated against release and touch down uncertainties, to guarantee the success of the landing strategy. More in detail, the effects of release uncertainty in terms of position and velocity have been investigated. The analysis shows that a important role is played by uncertainty in velocity, which must not be greater than few cm/s, while uncertainty in position can be accepted up to few tens of meters.

Figure 3 shows an example of dispersed release conditions. For mission design purpose, it is important to study the outcome of the dispersion analysis in terms of successful landing probability.

Table 1 shows the percentage of escaped trajectories after release dispersion. The results refer to a Monte Carlo simulation with 200000 release events simulated. As expected, success rate increases as the release altitude decreases.

After assessing the successful rate of the release strategy, it is important to study the outcome of the successful landing in terms of final landing point dispersion. Table 2 reports the latitude and longitude bands related to the resting point of MASCOT-2 on Didymoon, for different release altitude cases.

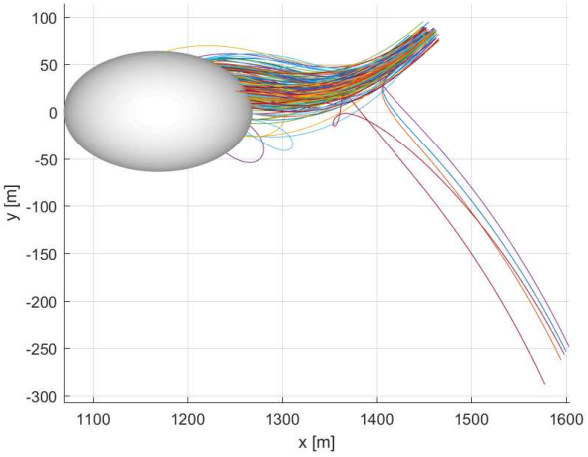

Fig. 3. Ballistic landing trajectory after release dispersion

Table 1. Escape probability from Didymoon

Release altitude [m]	Escaped trajectories [%]		
	After release	After touch down	TOT
100	1.14	0.00	1.14
150	1.26	0.00	1.26
200	3.18	0.01	3.19
250	5.79	0.04	5.83
300	6.03	0.32	6.35

The lander's time of flight (Tof) from release up to rest on Didymoon is also reported. Uncertainty range is included and specified according to a Gaussian 3-σ distribution.

Table 2. Landing dispersion on Didymoon's surface at rest: latitude/longitude bands and time of flight between release and rest

Release altitude [m]	Dispersion at rest [$\mu \pm 3\sigma$]		
	Lat [deg]	Long [deg]	Tof [h]
100	0.2 ± 32.5	23.3 ± 87.9	1.81 ± 0.95
150	0.0 ± 31.5	20.1 ± 66.7	2.19 ± 1.06
200	0.1 ± 32.9	19.7 ± 60.5	2.50 ± 1.21
250	-0.1 ± 36.6	20.5 ± 64.8	2.77 ± 1.41
300	0.1 ± 44.3	19.5 ± 86.0	2.95 ± 1.35

With reference to the case of 200m release altitude in Table 2, Figures 4, 5, 6, 7 shows the landing dispersion on the surface of Didymoon when the lander is at rest. More in detail, the latitude-longitude map is shown in Figure 4, while the three-dimensional view of all landing points on Didymoon's surface is shown in Figure 5. Latitude and longitude distributions are displayed, respectively, in Figure 6 and 7.

It must be highlighted that the dynamical behavior of the

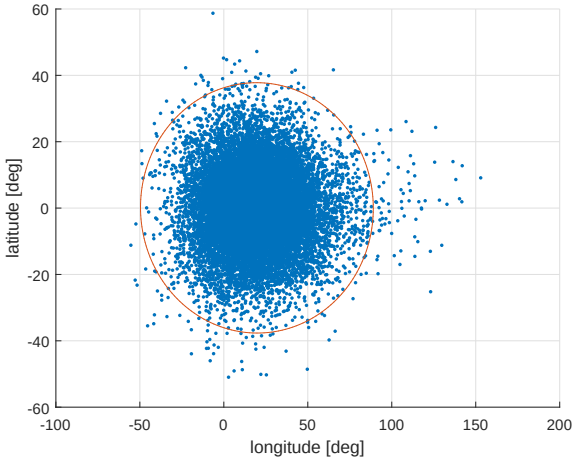

Fig. 4. Landing dispersion at rest for the case of 200 m altitude release: latitude-longitude map

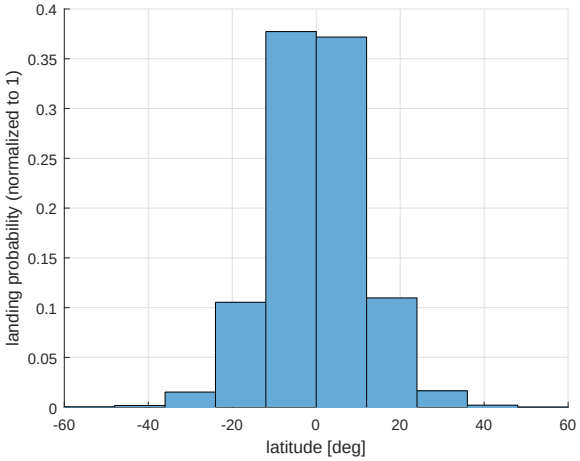

Fig. 6. Landing dispersion at rest for the case of 200 m altitude release: latitude distribution of points

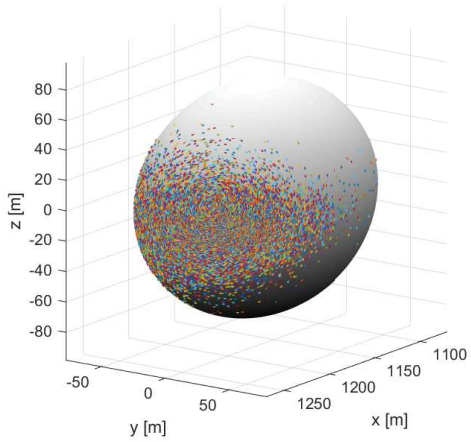

Fig. 5. Landing dispersion at rest for the case of 200 m altitude release: three-dimensional view of Didymoon

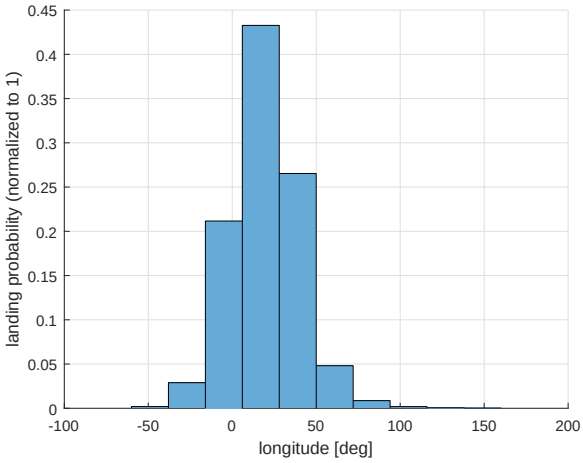

Fig. 7. Landing dispersion at rest for the case of 200 m altitude release: longitude distribution of points

lander after touch down is heavily dependent on the choice of the restitution coefficient η, defined in section 4. Within the assumptions currently applied at the present stage of MASCOT-2 release design process, the results shows that the landing region can be estimated. Although the uncertainty latitude-longitude region is quite high (on the order of tens of degrees), important information can be derived: it can be stated that the lander will come to a rest in the hemisphere of Didymoon opposite to Didymain.

6. CONCLUSION

Results show that the extremely low gravity environment does not guarantee the lander to stay on the surface after touch down, but MASCOT-2 will most likely bounce until reaching a stable position of Didymoon. Successful landing probability is assessed for the case of study and landing dispersion is evaluated. Compared to classical Keplerian solutions, three-body dynamics are found to be effective to lower the risk of rebounding on the surface of the secondary, and to increase the safety of the overall release maneuver to be performed by AIM.

As mentioned, the results and analysis here presented are part of the on-going AIM mission design process. Results might change during the AIM design due to updated requirements or updated reference model available on Didymos system.

7. ACKNOWLEDGEMENT

The work here presented has been performed by Politecnico di Milano under ESA contract during the phase A of AIM design, in consortium with OHB System AG and Spin.Works.

8. REFERENCES

[1] A Galvez, I Carnelli, M Fontaine, and C Corral Van Damme, "Asteroid impact mission (aim) & deflection assessment: an opportunity to understand impact dynamics and modelling," in *Proceedings of the European Planetary Science Congress*, Madrid, Spain, 2012.

[2] M Kueppers, I Carnelli, A Galvez, K Mellab, P Michel, and AIM Team, "The asteroid impact mission (aim)," in *Proceedings of the European Planetary Science Congress*, Nantes, France, 2015.

[3] A Galvez, I Carnelli, M Khan, W Martens, P Michel, S Ulamec, and A Hriscu, "Asteroid investigation mission: the european contribution to the aida eu-us cooperation," in *Proceedings of the 24th International Symposium on Space Flight Dynamics*, Laurel, MD, USA, 2014.

[4] P Michel, A Cheng, A Galvez, C Reed, I Carnelli, P Abell, S Ulamec, A Rivkin, J Biele, and N Murdoch, "Aida: Asteroid impact and deflection assessment," *Highlights of Astronomy*, 2009.

[5] A F Cheng, P Michel, C Reed, A Galvez, and I Carnelli, "Aida: Asteroid impact & deflection assessment," in *Proceedings of the IAA Planetary Defense Conference*, Flagstaff, AZ, USA, 2013.

[6] A.F Cheng, J Atchison, B Kantsiper, A.S Rivkin, A Stickle, C Reed, A Galvez, I Carnelli, P Michel, and S Ulamec, "Asteroid impact and deflection assessment mission," *Acta Astronautica*, vol. 115, pp. 262–269, 2015.

[7] P Scheirich and P Pravec, "Modeling of lightcurves of binary asteroids," *Icarus*, vol. 200, pp. 531–547, 2009.

[8] A F Cheng, P Michel, C Reed, A Galvez, and I Carnelli, "Dart: Double asteroid redirection test," in *Proceedings of the European Planetary Science Congress*, Madrid, Spain, 2012.

[9] A Cheng, A Stickle, J Atchison, O Barnouin, A Rivkin, P Michel, S Ulamec, and AIDA Team, "Asteroid impact and deflection assessment mission: Double asteroid redirection test (dart)," in *Proceedings of the 4th IAA Planetary Defense Conference*, Frascati, Italy, 2015.

[10] A M Stickle, J A Atchison, O S Barnouin, A F Cheng, C M Ernst, Z Fletcher, D C Richardson, and A S Rivkin, "Modeling momentum transfer from the dart spacecraft impact into the moon of didymos," in *Proceedings of the 4th IAA Planetary Defense Conference*, Frascati, Italy, 2015.

[11] A Herique and W Kofman, "Definition of the consert / rosetta radar performances," in *Proceedings of the CEOS SAR Workshop*, Tokyo, Japan, 2001.

[12] D Kolbe and R Best, "The rosetta mission," *Acta Astronautica*, vol. 41, pp. 569–577, 1997.

[13] E Heggy, E M Palmer, W Kofman, S M Clifford, K Righter, and A Hrique, "Radar properties of comets: Parametric dielectric modeling of comet 67p/churyumovgerasimenko," *Icarus*, vol. 221, pp. 925–939, 2012.

[14] J Biele and S Ulamec, "Capabilities of philae, the rosetta lander," *Space Science Review*, vol. 138, pp. 275–289, 2008.

[15] S Ulamec, J Biele, P-W Bousquet, P Gaudon, K Geurts, T-M Ho, C Krause, C Lange, R Willnecker, L Witte, Philae, and MASCOT teams, "Landing on small bodies: From the rosetta lander to mascot and beyond," *Acta Astronautica*, vol. 93, pp. 460–466, 2014.

[16] A Tsuchiyama, M Uesugi, T Matsushima, T Michikami, T Kadono, T Nakamura, K Uesugi, T Nakano, R Sandford, S A nad Noguchi, T Matsumoto, J Matsuno, T Nagano, Y Imai, A Takeuchi, Y Suzuki, T Ogami, J Katagiri, M Ebihara, T R Ireland, F Kitajima, K Nagao, H Naraoka, T Noguchi, R Okazaki, H Yurimoto, M E Zolensky, T Mukai, M Abe, T Yada, A Fujimura, M Yoshikawa, and J Kawaguchi, "Three-dimensional structure of hayabusa samples: Origin and evolution of itokawa regolith," *Science*, vol. 333, no. 6046, pp. 1125–1128, 2011.

[17] F Ferrari and M Lavagna, "Asteroid impact monitoring mission: Mission analysis and innovative strategies for close proximity maneuvering," in *Proceedings of the 4th IAA Planetary Defense Conference*, Frascati, Italy, 2015.

[18] F Ferrari and M Lavagna, "Asteroid impact mission: A possible approach to design effective close proximity operations to release mascot-2 lander," in *Proceedings of AIAA/AAS Astrodynamics Specialist Conference*, Vail, CO, USA, 2015.

[19] F Ferrari and M Lavagna, "Consolidated phase a design of asteroid impact mission: Mascot-2 landing on binary asteroid didymos," in *Proceedings of AAS/AIAA Space Flight Mechanics Meeting*, Napa, CA, USA, 2016.

[20] V Szebehely, *Theory of Orbits: The Restricted Problem of Three Bodies*, Academic Press, New York and London, 1967.

[21] H Schaub and J L Junkins, *Analytical Mechanics of Aerospace Systems*, American Institute Of Aeronautics & Astronautics, 2002.

[22] W S Koon, M W Lo, J E Marsden, and S D Ross, *Dynamical Systems, the Three Body Problem and Space Mission Design*, World Scientific, 2006.

[23] R A Werner and D J Scheeres, "Exterior gravitation of a polyhedron derived and compared with harmonic and mascon gravitation representations of asteroid 4769 castalia," *Celestial Mechanics and Dynamical Astronomy*, vol. 65, pp. 313–344, 1997.

[24] D J Scheeres, "Dynamics about uniformly rotating triaxial ellipsoids: Applications to asteroids," *Icarus*, vol. 110, pp. 225–238, 1994.